

## **Drug Solubilization by Mixtures of Cyclodextrins**

Additive and Synergistic Effects

Schönbeck, Jens Christian Sidney; Gaardahl, Karina; Houston, Bryan

*Published in:*  
Molecular Pharmaceutics

*DOI:*  
[10.1021/acs.molpharmaceut.8b00953](https://doi.org/10.1021/acs.molpharmaceut.8b00953)

*Publication date:*  
2019

*Document Version*  
Peer reviewed version

*Citation for published version (APA):*

Schönbeck, J. C. S., Gaardahl, K., & Houston, B. (2019). Drug Solubilization by Mixtures of Cyclodextrins: Additive and Synergistic Effects. *Molecular Pharmaceutics*, 16(2), 648-654.  
<https://doi.org/10.1021/acs.molpharmaceut.8b00953>

### **General rights**

Copyright and moral rights for the publications made accessible in the public portal are retained by the authors and/or other copyright owners and it is a condition of accessing publications that users recognise and abide by the legal requirements associated with these rights.

- Users may download and print one copy of any publication from the public portal for the purpose of private study or research.
- You may not further distribute the material or use it for any profit-making activity or commercial gain.
- You may freely distribute the URL identifying the publication in the public portal.

### **Take down policy**

If you believe that this document breaches copyright please contact [rucforsk@kb.dk](mailto:rucforsk@kb.dk) providing details, and we will remove access to the work immediately and investigate your claim.

# Drug Solubilization by Mixtures of Cyclodextrins: Additive and Synergistic Effects

Christian Schönbeck<sup>a,\*</sup>, Karina Gaardahl<sup>a</sup> and Bryan Houston<sup>a</sup>

<sup>a</sup> Department of Science and Environment, Roskilde University, Universitetsvej 1, DK-4000, Roskilde, Denmark

\*Corresponding author:

E-mail: jechsc@ruc.dk, Telephone: +45 46742345

Department of Science and Environment

Roskilde University

Universitetsvej 1

DK-4000 Roskilde

Denmark

## Abstract

Cyclodextrins are popular drug solubilizers, but the use of the natural cyclodextrins is hampered by their tendency to co-precipitate with the drug. To understand and overcome such problems, we have studied the solubility of dexamethasone in the presence of natural  $\beta$ -cyclodextrin and  $\gamma$ -cyclodextrin, individually and in various combinations. Equilibrium models of the phase-solubility diagrams with individual cyclodextrins revealed that dexamethasone was solubilized as 1:1 complexes, but formation of insoluble higher-order complexes set an upper limit to the concentration of solubilized dexamethasone. This limit could be raised from 8 mM to 17 mM by using combinations of the two cyclodextrins, as their solubilizing properties were additive in some regions of the phase-solubility diagram and synergistic in other regions. The additive effects arise from the additivity of solubilities – same phenomenon contributes to the good solubilizing properties of many modified cyclodextrins. The synergistic effects, however, could not be explained. The results open up for an increased use of the natural cyclodextrins as an improved alternative to modified cyclodextrins.

**Keywords:** Cyclodextrin, Inclusion complex; Phase-solubility; Steroid

## Introduction

Cyclodextrins (CDs) are often used drug solubilizers due to their ability to form water-soluble inclusion complexes with a large variety of drug molecules.<sup>1</sup> The cyclic structure of CDs consists of typically 6, 7, or 8 linked glucose monomers, termed  $\alpha$ ,  $\beta$ , and  $\gamma$ CD, respectively. Depending on the diameter, CDs may encapsulate drug moieties of various sizes. In addition to these so-called natural CDs, a large number of chemically modified CDs have been synthesized, the most common being hydroxypropylated, sulfobutylated, and methylated CDs. These modified CDs have a higher aqueous solubility and an often improved toxicological profile compared to their parent CDs.<sup>2</sup> In contrast to the natural CDs, they are highly heterogeneous samples, containing a variety of CDs differing in the degree and pattern of substitution.

The drug-solubilizing properties of a given CD is often studied by phase-solubility (PS) analysis in which the concentration of dissolved drug is plotted against the amount of added CD.<sup>3,4</sup> There seems to be a general tendency for modified CDs to result in A-type PS profiles in which the concentration of dissolved drug increases monotonously with the amount of added CD. In contrast, the natural  $\beta$  and  $\gamma$ CD often exhibit B-type profiles in which the formed complexes have a limited solubility and precipitate from the solution.<sup>4</sup> Such behavior is problematic and may limit the use of natural  $\beta$  and  $\gamma$ CD. On the other hand, the natural CDs often have higher binding constants, meaning that less CD is required to solubilize a given amount of drug. This may be of importance in solid oral dosage forms where the bulk formulation preferably should be contained in a single tablet of limited size.<sup>5</sup> Further, the complex sample composition of the modified CDs may be a drawback in terms of sample characterization, batch-to-batch variations and related regulatory issues. In order to improve the use of the natural CDs, it is desirable to understand why they, in contrast to the modified CDs, have B-type profiles and to discover methods to overcome this problematic behavior.

It has previously been discovered that addition of small amounts of HP $\gamma$ CD to natural  $\gamma$ CD significantly improves the complexation efficiency of the latter.<sup>6</sup> This synergistic effect was speculated to be related to the formation of aggregates of CDs and their complexes,<sup>7</sup> but this hypothesis is difficult to prove due to the presumably short-lived and complex nature of the aggregates. The present work aims to shed light on the causes for the reported synergistic effects and to understand why the solubilizing properties of natural and modified CDs are so different. To keep things simple, the complex mixtures of modified CDs were avoided, and the solubilizing properties of two pure CDs,  $\beta$ CD and  $\gamma$ CD, were studied individually and in various mixing ratios. Dexamethasone (DX) was chosen as drug molecule as the reported synergistic effects were observed for this particular drug. Like most other steroids, DX is known to give B<sub>S</sub>-type PS profiles with natural  $\beta$  and  $\gamma$ CD and A<sub>L</sub>-type profiles with modified CDs.<sup>8-13</sup> Further, the molecular mechanisms behind the PS diagram of  $\gamma$ CD with the structurally similar steroid hydrocortisone were recently described in detail.<sup>14</sup> It seems feasible to obtain a similar mechanistic understanding of the current system consisting of one drug and two CDs. Such understanding may be extended to complex mixtures of CDs, like the modified CDs, and may explain the reported synergistic effects. Ultimately, we hope this study can contribute to overcoming the problems associated with the low solubility of many drug complexes with natural  $\beta$  and  $\gamma$ CD.

## Theoretical Background

PS diagrams are constructed by measuring the total solubility of a fixed amount of solid substrate ( $S$ , in this work DX) in a medium containing increasing amounts of solubilizer or ligand ( $L$ , in this work CD). The theoretical framework for the various types of PS diagrams were laid out by Higuchi and Connors in 1965<sup>3</sup> and later developed for several special cases of  $B_S$ -type PS diagrams.<sup>14–16</sup> The interested reader is referred to these references for details; the present text only highlights the main points.

$B_S$ -type PS profiles occur when one of the formed complexes has a limited solubility and precipitates from the solution. In the present case, DX forms soluble 1:1 complexes and insoluble higher-order complexes with both CDs. As shown in Figure 2, this gives rise to three regions in the PS diagram. In region I, the DX concentration in the liquid phase increases linearly with increasing amounts of CD. In region II, all concentrations are constant as the precipitate consists of two solid phases of respectively precipitated higher-order complex and solid DX. This maintains constant concentrations of all dissolved species. Region III occurs when enough CD has been added such that all solid DX is solubilized or has precipitated as higher-order complexes. The absence of solid DX permits the concentration of free DX to go below its intrinsic solubility,  $S_0$ , and continued addition of CD will gradually deplete DX from the solution and precipitate it as higher-order complex.

The mathematical modelling rests on a set of equations based on mass conservation and chemical equilibria. The relevant mass conservations relates to the total concentrations of DX ( $S_{eq}$ ) and CD ( $L_{eq}$ ) in solution:

$$S_{eq} = [S] + [LS] \quad (1)$$

$$L_{eq} = [L] + [LS] \quad (2)$$

and to the distribution of molecules between solution and precipitate:

$$S_t = S_{eq} + y \times L_x S_y^{prec} \quad (4)$$

$$L_t = L_{eq} + x \times L_x S_y^{prec} \quad (5)$$

$S_t$  and  $L_t$  are the total amounts of DX and CD added to the vial, and  $L_x S_y^{prec}$  is the amount of higher-order complexes in the precipitate.

The concentration of 1:1 complexes,  $[LS]$ , is governed by the binding constant:

$$[LS] = K \times [L] \times [S] \quad (6)$$

and the precipitation of higher-order complexes is determined by the solubility product:

$$K_s^{xy} = [L]^x [S]^y \quad (7)$$

Solving this system of equations with the region-specific constraints yields the concentrations of the dissolved species, as shown in the Supporting Information. It is important to note that the model assumes that no higher-order complexes ( $x > 1$  and/or  $y > 1$ ) are present in the liquid phase. Such complexes may only be present in the solid phase. For this reason, no concentrations of higher-order complexes appear in the equations and no equilibrium constant for the formation of higher-order complexes in the liquid phase is defined. These are omitted from the model as the presently studied systems turned out to behave similarly to a previous study of hydrocortisone and  $\gamma$ CD in which no higher-order complexes were present in solution.<sup>14</sup>

## Experimental Section

### Chemicals

$\beta$ -cyclodextrin (purity  $\geq 97\%$ ) and  $\gamma$ -cyclodextrin (purity  $\geq 98\%$ ) were purchased from Sigma-Aldrich. The water content of the cyclodextrins ( $11.26 \pm 0.08\text{wt}\%$  for  $\beta$ CD,  $9.07 \pm 0.05\text{wt}\%$  for  $\gamma$ CD) was determined from the mass loss upon drying. Dexamethasone (96% purity) was from Acros Organics. Milli-Q water was used for all solutions.

### Isothermal titration calorimetry

To determine the binding constants of DX to each of the two CDs calorimetric titrations were made on a VP-ITC (Malvern Panalytical, Malvern, UK) with a 1.4257 ml reaction cell. 3 mM aqueous solutions of CD were titrated into 0.15 mM aqueous solutions of DX at 10, 25, 40, and 55 °C at a stirring speed of 310 rpm. Each titration consisted of 29 injections, each injection having a volume of 10  $\mu$ L. The resulting enthalpograms were analyzed by a global fitting procedure using in-house Matlab scripts to yield the binding constant, stoichiometry, binding enthalpy, and change in heat capacity.<sup>17</sup>

### Experimental generation of phase-solubility diagrams

For each phase-solubility diagram, a constant amount of solid DX was weighed and transferred to 2 ml Eppendorf tubes. 14.3 mg (35 mM) DX was used for the PS diagrams with individual CDs and 16.4 mg (40 mM) for the experiments with mixtures of CDs. Varied amounts of CD(s) and 1 ml of Milli-Q water was added to each tube. The tubes were agitated for at least 6 days at 400 rpm on a shaking table thermostatted at 25 °C. After equilibration, the solid particles were spun down and



the supernatant was removed using a plastic Pasteur pipette. After filtering and appropriate dilution, the concentration of DX in the supernatant was measured using an Agilent 1100 Series HPLC. CD and DX were separated on a C18 column using 70% methanol/water as mobile phase, having a flow of 0.8 ml/min. 20 µl of each sample was injected once with a run time of 8 min. DX was eluted after 5.9 min and its concentration was quantified from the absorbance at 250 nm.

The tubes with the precipitate were dried overnight in vacuum at 55 °C and weighed to determine the contents of DX and CD. The amount of DX in the precipitate could be determined as the difference between added DX and DX in the supernatant. The remaining mass of the precipitate would then be CD. Then the amount of CD in the supernatant could be determined as the difference between added CD and CD in the precipitate. The errors resulting from this indirect determination of the CD concentrations were estimated from a similar treatment of the samples that only contained DX and water. These indicated that the CD concentrations could be determined with an error of less than 1 mM.

#### Differential scanning calorimetry

For each analyzed sample, 2-4 mg of dried precipitate was heated from 50 to 270 °C in aluminium pans at a rate of 20 °C/min on a Pyris 1 DSC (Perkin Elmer, Waltham, MA).

## Results

Prior to exploring the solubilizing properties of mixtures of  $\beta$  and  $\gamma$ CD, the solubilizing properties of individual CDs were characterized by PS analysis. Mathematical modelling of the PS diagrams confirmed a mechanistic model in which the CDs formed soluble 1:1 complexes and insoluble higher-order complexes. To verify the mathematical model, some of the parameters were determined by independent experiments. The 1:1 binding constants,  $K$ , were determined by isothermal titration calorimetry, and the intrinsic solubility of DX,  $S_0$ , was determined by solubility measurements.

### Isothermal titration calorimetry

Binding constants for the 1:1 complexes of DX with  $\gamma$ CD and  $\beta$ CD were accurately determined by ITC. In principle, a single titration provides the binding constant,  $K$ , the binding enthalpy,  $\Delta H$ , and the stoichiometry of the complex,  $N$ . A more robust method is to perform titrations at different temperatures and conduct a global fit of all titrations.<sup>17</sup> This method employs an additional fitting parameter, the change in heat capacity ( $\Delta C_p$ ), and ensures that the obtained results are consistent with fundamental thermodynamic relations. The results from the titrations of DX with  $\gamma$ CD and  $\beta$ CD are shown in Figure 1. In both cases, the stoichiometry was very close to 1, indicating the formation of 1:1 complexes with both CDs. The binding constant for  $\gamma$ CD ( $13.9 \text{ mM}^{-1}$ ) was more than twice as high as for  $\beta$ CD ( $5.7 \text{ mM}^{-1}$ ). The measured binding constant for the  $\beta$ CD:DX complex was similar to reported values measured under similar conditions ( $4.7 \text{ mM}^{-1}$ <sup>10</sup>,  $6.2 \text{ mM}^{-1}$ <sup>18</sup>,  $7.4 \text{ mM}^{-1}$ <sup>19</sup>). For the  $\gamma$ CD:DX complex, the measured binding constant differed significantly from previously reported values determined by phase-solubility analysis ( $27 \text{ mM}^{-1}$ <sup>10</sup>,  $1.2 \text{ mM}^{-1}$ <sup>6</sup>). The presently reported values are assumed to possess a higher accuracy due to the employed global

fitting procedure. The large number of data points and the low degree of correlation between the fitting parameters yields a precise estimate of the binding constant, as evidenced by the statistics in Figure 1.

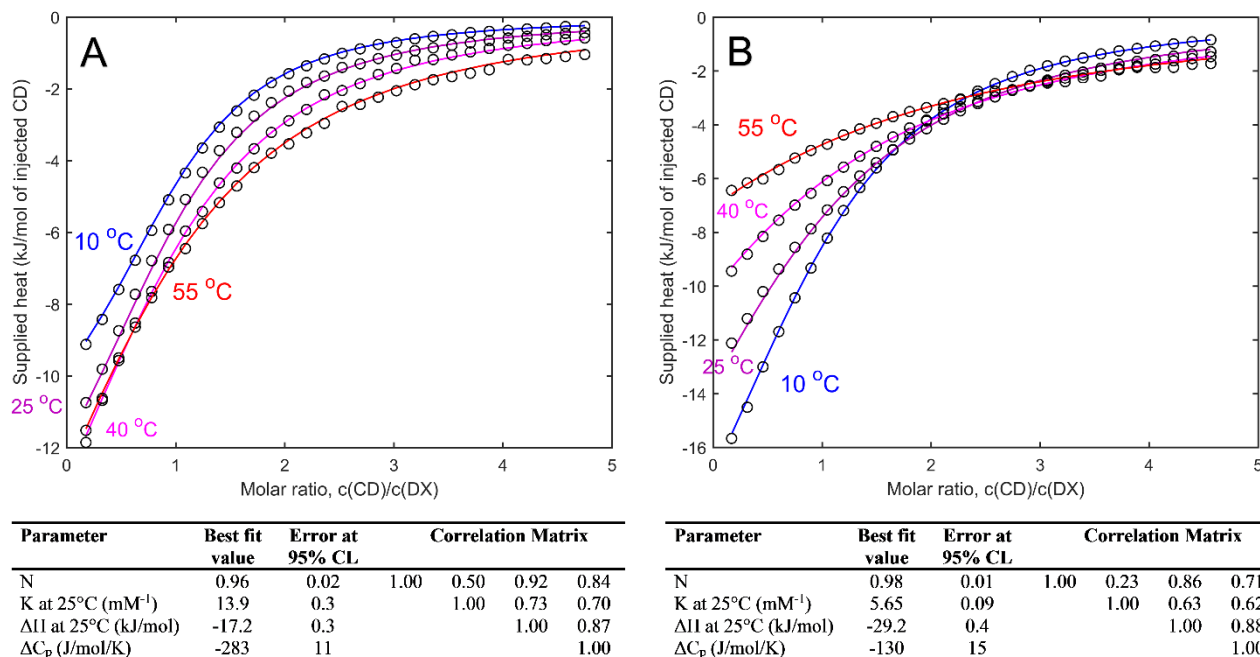


Figure 1 Enthalpograms from the titration of DX with  $\gamma$ CD (A) and  $\beta$ CD (B) conducted at 10°C, 25°C, 40°C, and 55°C. The parameters obtained from the global fit to the experiments are listed in the tables along with their statistics.

### Dexamethasone solubilized by $\gamma$ -cyclodextrin

The PS diagram for DX solubilized by  $\gamma$ CD was generated by adding a constant amount of solid DX, corresponding to 32.3 mM, to each vial and measuring the equilibrium concentration of DX in the aqueous phase. In the absence of  $\gamma$ CD, the intrinsic solubility of DX was determined to 0.164 mM  $\pm$  0.005 mM ( $\pm$ SD,  $n = 3$ ). As the concentration of  $\gamma$ CD in the added aqueous solvent increased, the amount of solubilized DX first increased linearly, then reached a plateau, followed by a sharp decrease. The resulting B<sub>S</sub>-type PS diagram is shown in Figure 2. From the length of region II the precipitation stoichiometry was determined to 1.48,<sup>3</sup> thus indicating that  $\gamma$ CD and DX

precipitated in a ratio of three  $\gamma$ CDs to two DX molecules. It therefore seems appropriate to model the experimental data using a 3:2 model in which  $x$  and  $y$  in eq. 7 are 3 and 2, respectively. The black line in Figure 2 shows the prediction of the 3:2 model. Out of the three parameters that determines the shape of the model prediction, two of the parameters,  $K$  and  $S_0$ , had already been determined by ITC and solubility measurements, respectively. The third parameter  $K_S^{32}$  was determined from the height of the plateau in region II ( $6.95 \pm 0.09$  mM) using eq. 8 (derived as eq. S5 in the Supporting Information):

$$K_S^{23} = \frac{(S_{eq}-S_0)^3}{K^3 \times S_0} \quad (8)$$

where  $S_{eq}$  is the height of the plateau. This yields  $K_S^{32} = 0.78$  mM<sup>5</sup>.

Figure 2 also shows the experimentally determined concentrations of CD in the liquid phase along with the prediction of the 3:2 model, using the same parameters as before. Due to the indirect determination of CD concentration from the mass of the precipitate these data points might be imprecise. It was not possible to determine the CD concentration directly by the UV-VIS detector in the HPLC system as the absorptivity of CDs is too low. It is possible, however, that direct determination of the CD concentrations by other detectors such as a charged aerosol detector<sup>20</sup> would have resulted in even better agreement between model and experiment. Nevertheless, the observed agreement clearly indicates that the model is plausible. This means that DX predominantly exists in solution as 1:1 complexes with  $\gamma$ CD and precipitates in a 3:2  $\gamma$ CD:DX ratio at high concentrations of  $\gamma$ CD.

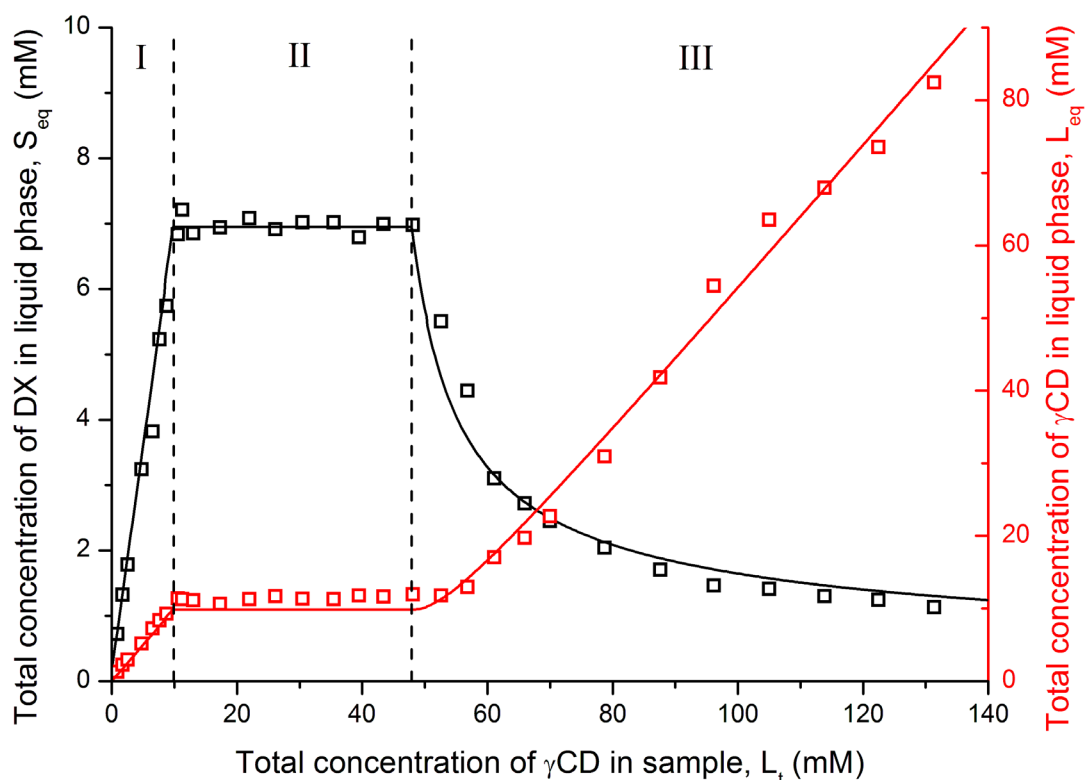


Figure 2 Experimental phase-solubility diagram of DX solubilized by  $\gamma$ CD (black squares, left axis) and total concentration of  $\gamma$ CD in liquid phase (red squares, right axis). Solid lines are generated by the 3:2 model, using the following parameters:  $S_0 = 0.164$  mM,  $K = 13.5$  mM<sup>-1</sup>, and  $K_S^{32} = 0.78$  mM<sup>5</sup>.

### Dexamethasone solubilized by $\beta$ -cyclodextrin

As for  $\gamma$ CD, the solubilization of DX by  $\beta$ CD also resulted in a B<sub>S</sub>-type PS diagram (Figure 3) but with a second plateau which will be termed region IIA. In region II, the precipitate consists of two solid phases: pure DX and precipitated higher-order complex. In region IIA, the solubility of  $\beta$ CD was reached, and the precipitate consisted of a solid phase of pure  $\beta$ CD and another solid phase of precipitated higher-order complex. The length of the region II plateau indicated that  $\beta$ CD and DX precipitated in a ratio of 2:1 (CD to DX), and therefore the data were modeled by a 2:1 model in which DX is solubilized as 1:1 CD complexes and precipitated as 2:1 complexes. In addition to the

1:1 binding constant and the intrinsic solubility of DX, which were determined by ITC and solubility measurements, the model employs the 2:1 CD:DX solubility product,  $K_S^{21}$ . Further, to describe region IIA, the intrinsic solubility of  $\beta$ CD,  $L_0$ , was set to the previously reported value of 16.3 mM at 25°C.<sup>21</sup>

The value of  $K_S^{21}$  can be determined from the height of the region II plateau, as was done for  $\gamma$ CD, but due to the more precise determination of the plateau in region IIA ( $4.42 \pm 0.06$  mM), this value was used to determine  $K_S^{21}$  according to eq. 8 (derived as eq. S10 in the SI) where  $L_0$  is the intrinsic solubility of  $\beta$ CD:

$$K_S^{21} = \frac{S_{eq} \times L_0^2}{K \times L_0 + 1} \quad (9)$$

yielding  $K_S^{21} = 12.6 \text{ mM}^3$ . The resulting plot of the 2:1 model generally revealed good agreement with the experimental data (Figure 3). In region I, however, there seemed to be a slight systematic deviation between the model and the experimental data. Linear regression to the data points in region I yielded a slope of 0.431, translating into a binding constant of  $4.62 \text{ mM}^{-1}$ .<sup>3</sup> This is a little lower than that determined by ITC but still within reasonable agreement, especially considering the range of previously reported values.

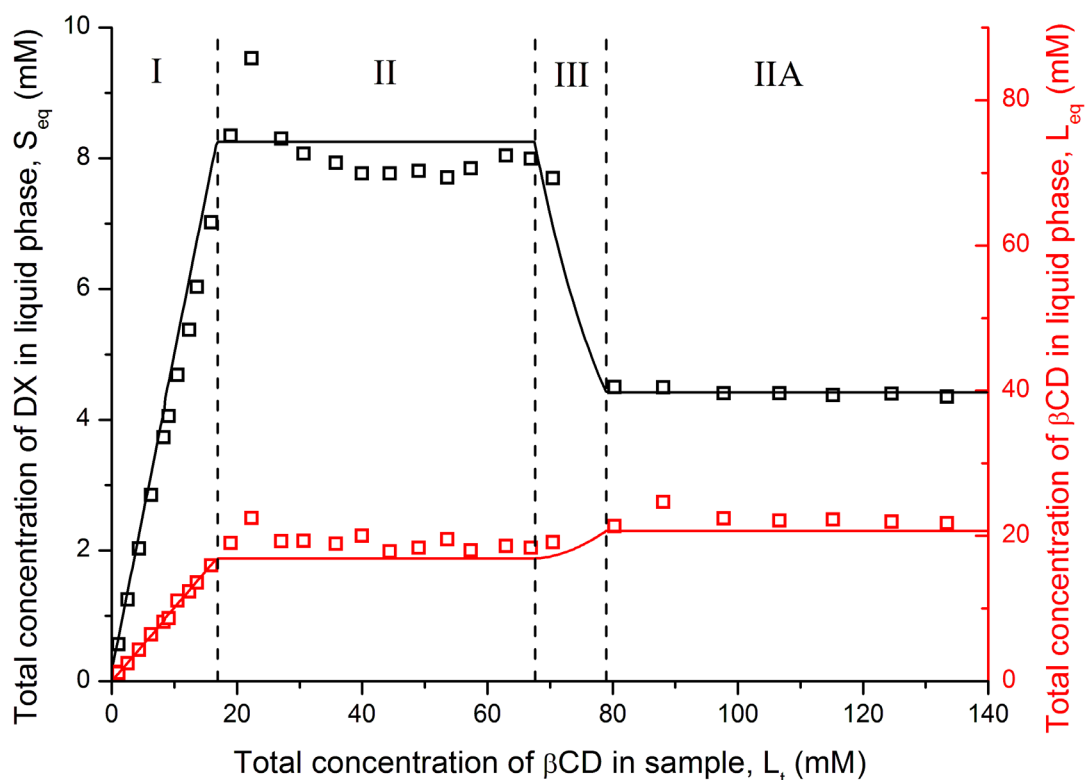


Figure 3 Experimental phase-solubility diagram of DX solubilized by  $\beta$ CD (black squares, left axis) and total concentration of  $\beta$ CD in liquid phase (red squares, right axis). Solid lines are generated by the 2:1 model, using the following parameters:  $S_0 = 0.164$  mM,  $K = 5.65$  mM<sup>-1</sup>,  $K_S^{21} = 12.6$  mM<sup>3</sup>, and  $L_0 = 16.3$  mM.

### Solubility of dexamethasone in mixtures of $\beta$ -cyclodextrin and $\gamma$ -cyclodextrin

The above results convincingly show that the  $B_S$ -type PS diagrams of DX with either  $\beta$ CD or  $\gamma$ CD can be accounted for by equilibrium models where DX is solubilized by formation of 1:1 complexes with the CDs but precipitates in a 3:2 or 2:1 CD:DX ratio. Precipitation sets in once the concentrations of uncomplexed CD and DX exceed the solubility product of the precipitate. The thorough understanding of these individual systems should in principle enable a prediction of the solubilizing properties of mixtures of  $\beta$ CD or  $\gamma$ CD, assuming that no other equilibria are present.

This will be explored in the following where the solubilizing properties of the mixtures are presented and discussed.

### Additive effects in region I

In region I there is no precipitation of complexes, and the precipitate consists exclusively of solid DX. This definition was used to determine which of the mixed samples belonged to region I. The gravimetric analysis of the precipitate could clearly distinguish between samples with and without precipitated complexes. The concentration of dissolved DX is shown in Figure 4A as a function of the total amount of added  $\beta$  and  $\gamma$ CD. The CDs were mixed in various ratios with concentrations ranging from 0-25 mM for  $\beta$ CD and 0-13 mM for  $\gamma$ CD. These ranges extend slightly into region II of the individual PS diagrams.

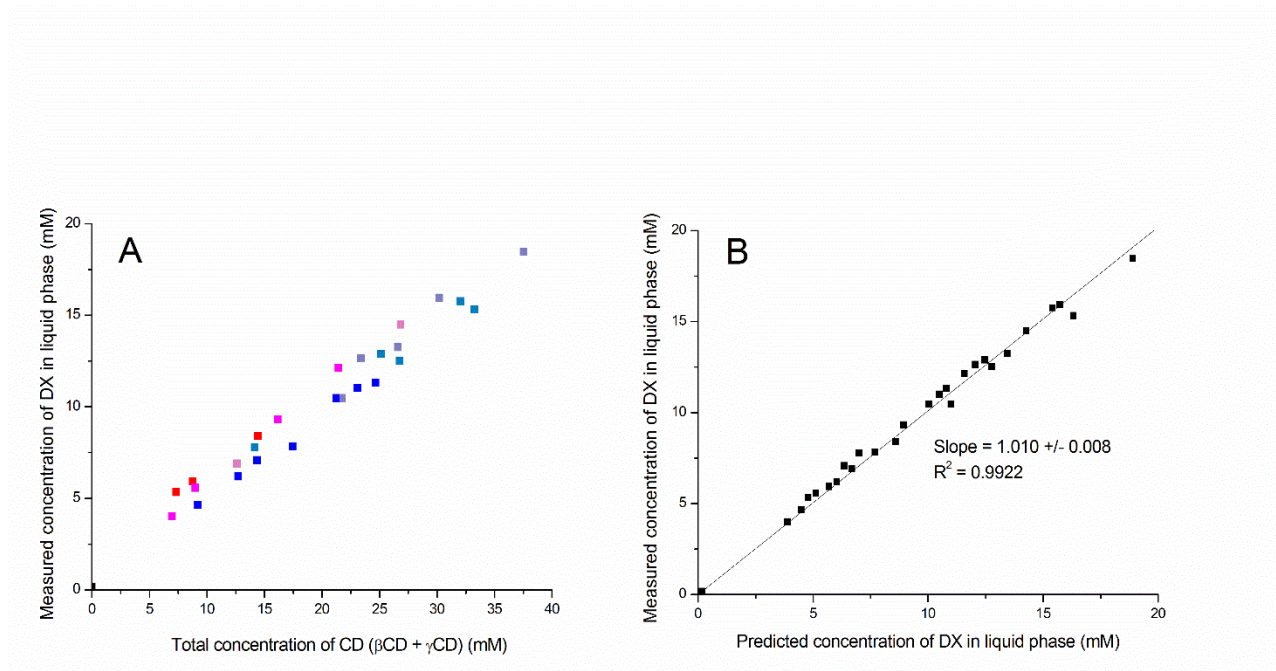


Figure 4 A) The total concentration of DX as a function of the total concentration of  $\beta$ CD and  $\gamma$ CD. The color code indicates the ratio of  $\gamma$ CD to  $\beta$ CD, ranging from dark blue for 100%  $\beta$ CD to red for 100%  $\gamma$ CD. B) Measured DX concentration vs predicted concentration. The slope of the regression line indicates excellent agreement between measured and predicted concentration of DX in the presence of  $\beta$ CD and  $\gamma$ CD.



As seen on Figure 4A the concentration of DX increases linearly up to a total CD concentration of around 35 mM. At this point, the DX concentration reaches 18 mM which is more than twice as high as in the experiments with the individual CDs. There is some scatter on the plot which is expected as the DX solubility is not unequivocally given by the total CD concentration but depends on the relative amounts of  $\beta$ CD or  $\gamma$ CD. Since  $\gamma$ CD is a more efficient solubilizer than  $\beta$ CD, samples with a higher ratio of  $\gamma$ CD to  $\beta$ CD can solubilize more DX, even if the total CD concentration is the same.

If the presence of two different kinds of CDs does not result in any new species, such as new types of complexes or aggregates, the total concentration of solubilized DX should be equal to the sum of free DX and DX complexed with  $\beta$ CD and  $\gamma$ CD:

$$DX_{eq} = [DX] + [\beta CD: DX] + [\gamma CD: DX] \quad (10)$$

This can be expressed as:

$$DX_{eq} = S_0 + \frac{K_\beta S_0}{1 + K_\beta S_0} \beta CD_t + \frac{K_\gamma S_0}{1 + K_\gamma S_0} \gamma CD_t \quad (11)$$

where  $K_\beta$  and  $K_\gamma$  are the 1:1 binding constants, and  $\beta CD_t$  and  $\gamma CD_t$  are the amounts of added CDs, expressed as concentrations. There was a small difference between the binding constants determined by ITC and those determined from region I of the individual PS diagrams. Insertion of the latter into eq. 11 yields an excellent agreement between the observed and predicted concentrations, as shown in Figure 4B. Using the ITC values, the predicted concentrations become around 8% larger than the measured concentrations. The excellent agreement between observations and predictions shows that the solubilizing effects of  $\beta$  and  $\gamma$ CD in region I are additive.

### Phase-solubility diagram with constant amount of $\gamma$ CD and varied amount of $\beta$ CD

To investigate the combined effects of  $\beta$  and  $\gamma$ CD in the other regions of the PS diagram, DX was dissolved in a series of CD mixtures containing a fixed amount of  $\gamma$ CD (20 mM) and varied concentrations of  $\beta$ CD. The 20 mM of  $\gamma$ CD was chosen well beyond the transition from region I to region II in order to avoid super-saturation which tends to occur close to the transition point (see Figures 2 and 3). All samples were therefore expected to contain precipitated 3:2  $\gamma$ CD:DX complexes and were thus in region II or III with respect to  $\gamma$ CD. With respect to  $\beta$ CD, the samples ranged from region I, at low concentrations of  $\beta$ CD, to region IIA at high concentrations of  $\beta$ CD, as seen in Figure 5.  $\beta$ CD at low concentrations solubilizes DX as a 1:1 complex and then precipitate as a 2:1 complex once the solubility product,  $K_S^{21}$ , is reached (region II). Additional amounts of  $\beta$ CD depletes the solid DX, leading to a decrease in the amount of dissolved DX (region III). The decrease in region III is not as steep as in the PS diagrams of the individual CDs, since the precipitation of DX as solid  $\beta$ CD complexes is partially countered by dissolution of solid  $\gamma$ CD complexes. Once the concentration of free  $\beta$ CD exceeds the intrinsic solubility of  $\beta$ CD the plateau of region IIA starts.

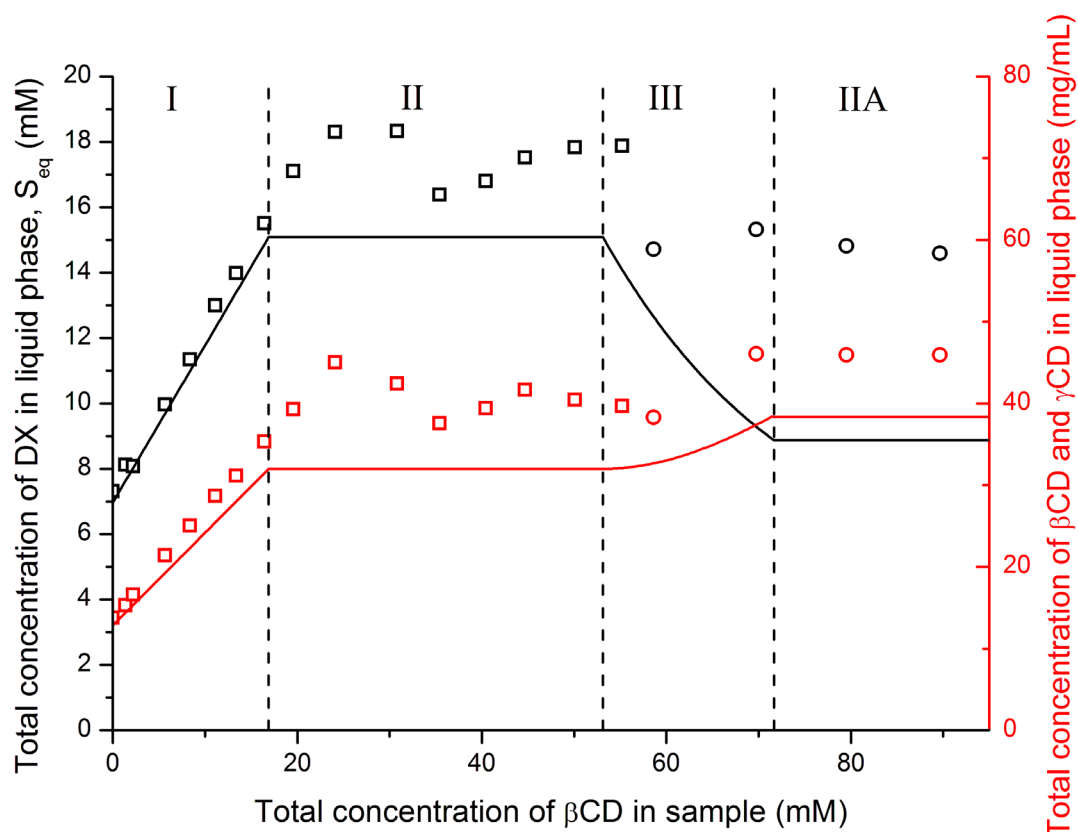


Figure 5 Solubility of DX in samples containing 20.34 mM  $\gamma$ CD and varied amounts of  $\beta$ CD. Symbols denote experimental measurements. Solid lines are model predictions, using the same parameters as for the modelling of the PS diagrams with individual CDs. Details of the modelling are provided as Supporting Information. The total concentration of dissolved CD (red symbols and lines, right axis) is given in mg/ml as the gravimetric method determines the total mass of CD, and this cannot be converted to number of moles without knowing the relative amounts of the two CDs. 40 mM DX was added to most samples but the round symbols came from samples where 21 mM DX was added. Increased amounts of added DX should only result in a linear shift along the x-axis, and the round symbols were shifted accordingly along the x-axis.

The measured concentrations of DX and CD are shown in Figure 5 along with the model predictions. The overall shape of the PS diagram, including the transitions between the regions, is in reasonable agreement with the model predictions, based on additive effects of  $\beta$  and  $\gamma$ CD. As expressed in eq. 10, additivity implies that the total DX concentration is the sum of free DX and that present as 1:1 complexes with  $\beta$  and  $\gamma$ CD. Although the overall shape seems correct, the DX solubilities and the concentrations of dissolved CD exceeds the predictions. This tendency is hardly seen in region I, but it seems clear in region II and is very pronounced in region IIA where the DX

concentration is almost twice as high as predicted. Region II and region IIA are discussed in the following.

#### Weak synergistic effect in region II

In region II, the additive model predicts the height of the plateau to be 15.1 mM but the experimental DX concentrations are around 18 mM. This seems to indicate a slight synergistic effect. There is a chance, however, that these discrepancies could be due to a slight deviation from the temperature at which the parameters were determined. To avoid such errors and get a statistically significant answer to whether there is a slight synergistic effect, three new samples were made in quadruplicate. The samples contained 40 mM DX and either  $\beta$ CD,  $\gamma$ CD, or a mix of the two CDs. All samples were processed exactly the same way with respect to temperature, equilibration time, and resting time before analysis. In the 4 identical samples containing 40 mM DX and 40 mM  $\beta$ CD, the concentration of solubilized DX was  $8.19 \pm 0.07$  mM which is quite close to the previously observed plateau value of 7.90 mM (Figure 3). In similar good agreement with previous results, the 4 identical samples containing 40 mM DX and 20 mM  $\gamma$ CD solubilized  $6.79 \pm 0.08$  mM DX. The 4 mixed samples containing 40 mM  $\beta$ CD and 20 mM  $\gamma$ CD, solubilized  $16.84 \pm 0.34$  mM DX. This is around 2 mM more than the combined effects of  $\beta$  and  $\gamma$ CD, thus confirming what seems to be a weak synergistic effect.

#### Strong synergistic effect in region IIA

The modelling in Figure 5 shows that two samples are inside region IIA. This region is characterized by the presence of pure solid  $\beta$ CD, the presence of which was confirmed by a small endothermic peak at 220-225°C in the DSC curves.<sup>22</sup> Solid  $\beta$ CD was also identified in the sample

right before region IIA (at 70 mM added  $\beta$ CD) but not in any other samples. The attribution of this peak to solid  $\beta$ CD is supported by its presence in all of the region IIA samples of the PS diagram with  $\beta$ CD where the peak area was roughly proportional to the amount of solid  $\beta$ CD. The additive model predicts a DX concentration of 8.9 mM but the measured concentrations were around 15 mM, clearly showing a strong synergistic effect.

## Discussion

The PS diagrams of DX with the individual CDs were well described by equilibrium models in which DX forms water-soluble 1:1 complexes with CD and precipitates as higher-order complexes. Precipitation takes place when the product of the concentrations exceeds the solubility product of the precipitate. For  $\beta$ CD, precipitation occurs when the total concentration of  $\beta$ CD exceeds 17 mM. At this point, the concentration of DX is 7.9 mM, and this is the maximum amount of DX that can be solubilized by  $\beta$ CD.  $\gamma$ CD can solubilize up to 7 mM DX, which requires addition of 10 mM  $\gamma$ CD. When both CDs are present, the solubilizing effects are additive, and the apparent solubility of DX can reach 17 mM. This is because the linearly increasing part of the PS diagram is extended, and precipitation does not occur until a total of more than 30 mM CD has been added. Most modified CDs, such as partially methylated, sulfobutylated and hydroxypropylated CDs, are complex mixtures containing hundreds of CD isomers and homologues. Each of these isomers may in principle precipitate with a drug, but as the concentration of each isomer is very low precipitation will not occur. This is probably the reason why modified CDs give A-type PS diagrams. Same phenomenon contributes to the increased solubility of modified CDs for which the solubility is the sum of the independent solubilities of its components.<sup>23</sup> The present work shows that this “multiple component effect” can be exploited to improve the solubilizing properties of the natural CDs, thereby expanding their usage.

Precipitation of complexes is not a problem that is limited to the natural CDs. All pure CDs may suffer from this limitation. For example, two promising neutral  $\beta$ CD thioethers with a strong affinity for steroids turned out to be poor solubilizers due to precipitation of complexes.<sup>24</sup> Mixtures of high-affinity CDs may to some extent alleviate such problems and form a strong-binding alternative to the conventional modified CDs.

The additive model assumes that the apparent solubility of DX is given as the sum of  $[DX]$ ,  $[\beta CD:DX]$  and  $[\gamma CD:DX]$  (eq. 10), and that these concentrations in turn are given by the complexation constants for the 1:1 complexes and the solubility products of the precipitated entities (eq. 6 and 7). In other words, the equilibria that describes the PS diagrams with the individual CDs are assumed to describe the solubility of DX when both CDs are present. In region I, when no CDs had precipitated, the combined effect of  $\beta$  and  $\gamma$ CD was well described by the additive model. In contrast, synergistic effects were observed in region II and region IIA of the PS diagram with the CD mixtures. This indicates that other equilibria than those described by equations 6 and 7 become relevant. We speculate that additional soluble species may form, for instance a 1:1:1 complex consisting of one DX molecule binding one  $\beta$ CD and one  $\gamma$ CD. Similarly, other solid phases may form, such as a solid phase containing DX and both of the CDs. The presence of two CDs opens up for the possibility of having several new species in solution and in the precipitate, some of which may explain the observed synergistic effects. A proper understanding of these effects may improve the pharmaceutical use of CDs as drug solubilizers.

## Conclusion

The B<sub>S</sub>-type phase-solubility diagrams of DX solubilized by either  $\beta$ CD or  $\gamma$ CD were described by an equilibrium model in which DX forms water-soluble complexes with a 1:1 stoichiometry and precipitates as higher-order complexes, having a stoichiometry of 2:1  $\beta$ CD:DX or 3:2  $\gamma$ CD:DX. The solubility products of the precipitating entities limits the amount of DX in solution to a maximum of 8 mM and 7 mM, when solubilized by respectively  $\beta$ CD and  $\gamma$ CD. The solubilizing properties of the CDs are additive, and when DX is solubilized by mixtures of the two CDs the highest obtainable concentration increases to 17 mM. The increased solubility is due to the additivity of the solubilities of the individual components. This phenomenon also explains why the commonly used modified CDs, which are mixtures of hundreds of isomers, give A-type phase-solubility diagrams with most drug molecules.

The phase-solubility diagram of DX with mixtures of  $\beta$ CD or  $\gamma$ CD reveals not only additive but also significant synergistic effects in some regions of the phase solubility diagram. This suggests the presence of additional species in solution, but this explanation is so far purely speculative.

## Acknowledgements

CS was supported by a grant (DFF – 5054-00173) from the Danish Council for Independent Research. The ITC experiments were conducted by bachelor students at Roskilde University: David Bartos, Nadia Hansen, Malene Pedersen, Kasper Larsen, and Emil Lund.

**Supporting Information.** Mathematical modeling of phase-solubility diagrams.



## References

- (1) Williams, H.; Trevaskis, N.; Charman, S.; Shanker, R.; Charman, W.; Pouton, C.; Porter, C. Strategies to Address Low Drug Solubility in Discovery and Development. *Pharmacol. Rev.* **2013**, *65*, 315–499.
- (2) Irie T., U. K. Pharmaceutical Applications of Cyclodextrins. III. Toxical Issues and Safety Evaluation. *J. Pharm. Sci.* **1997**, *86*, 147–162.
- (3) Higuchi, T.; Connors, K. A. Phase-Solubility Techniques. In *Advances In Analytical Chemistry and Instrumentation*; Reilley, C., Ed.; Interscience: New York, 1965; pp 117–212.
- (4) Brewster, M. E.; Loftsson, T. Cyclodextrins as Pharmaceutical Solubilizers. *Adv. Drug Deliv. Rev.* **2007**, *59*, 645–666.
- (5) Loftsson, T.; Brewster, M. E. Cyclodextrins as Functional Excipients: Methods to Enhance Complexation Efficiency. *J. Pharm. Sci.* **2012**, *101*, 3019–3032.
- (6) Jansook, P.; Loftsson, T.  $\gamma$ CD/HP $\gamma$ CD: Synergistic Solubilization. *Int. J. Pharm.* **2008**, *363*, 217–219.
- (7) Jansook, P.; Kurkov, S. V; Loftsson, T.; Taylor, M. J.; Tanna, S.; Sahota, T. Cyclodextrins as Solubilizers: Formation of Complex Aggregates. *J. Pharm. Sci.* **2010**, *99*, 719–729.
- (8) Müller, B. W.; Brauns, U. Solubilization of Drugs by Modified  $\beta$ -Cyclodextrins. *Int. J. Pharm.* **1985**, *26*, 77–88.
- (9) Müller, B. W.; Brauns, U. Change of Phase-Solubility Behavior by Gamma-Cyclodextrin Derivatization. *Pharm. Res.* **1985**, *2*, 309–310.
- (10) Uekama, K.; Fujinaga, T.; Hirayama, F.; Otagiri, M.; Yamasaki, M. Inclusion Complexations

- of Steroid Hormones with Cyclodextrins in Water and in Solid Phase. *Int. J. Pharm.* **1982**, *10*, 1–15.
- (11) Messner, M.; Kurkov, S. V.; Brewster, M. E.; Jansook, P.; Loftsson, T. Self-Assembly of Cyclodextrin Complexes: Aggregation of Hydrocortisone/Cyclodextrin Complexes. *Int. J. Pharm.* **2011**, *407*, 174–183.
  - (12) Jansook, P.; Moya-Ortega, M. D.; Loftsson, T. Effect of Self-Aggregation of  $\gamma$ -Cyclodextrin on Drug Solubilization. *J. Incl. Phenom. Macrocycl. Chem.* **2010**, *68*, 229–236.
  - (13) Thi, T. Do; Nauwelaerts, K.; Froeyen, M.; Baudemprez, L.; Van Speybroeck, M.; Augustijns, P.; Annaert, P.; Martens, J.; Van Humbeeck, J.; Van Den Mooter, G. Comparison of the Complexation between Methylprednisolone and Different Cyclodextrins in Solution by <sup>1</sup>H-NMR and Molecular Modeling Studies. *J. Pharm. Sci.* **2010**, *99*, 3863–3873.
  - (14) Schönbeck, C.; Madsen, T. L.; Peters, G. H.; Holm, R.; Loftsson, T. Soluble 1:1 Complexes and Insoluble 3:2 Complexes – Understanding the Phase-Solubility Diagram of Hydrocortisone and  $\gamma$ -Cyclodextrin. *Int. J. Pharm.* **2017**, *531*, 504–511.
  - (15) Zughul, M. B.; Badwan, A. A. Rigorous Analysis of S2L-Type Phase Solubility Diagrams to Obtain Individual Formation and Solubility Product Constants of Both SL-and S2L-Type Complexes. *Int. J. Pharm.* **1997**, *151*, 109–119.
  - (16) Zughul, M.; Badwan, A. SL2 Type Phase Solubility Diagrams, Complex Formation and Chemical Speciation of Soluble Species. *J. Incl. Phenom. Macrocycl. Chem.* **1998**, *31*, 243–264.
  - (17) Schönbeck, C.; Holm, R.; Westh, P. Higher Order Inclusion Complexes and Secondary Interactions Studied by Global Analysis of Calorimetric Titrations. *Anal. Chem.* **2012**, *84*,

2305–2312.

- (18) Mateen, R.; Hoare, T. Carboxymethyl and Hydrazide Functionalized  $\beta$ -Cyclodextrin Derivatives: A Systematic Investigation of Complexation Behaviours with the Model Hydrophobic Drug Dexamethasone. *Int. J. Pharm.* **2014**, *472*, 315–326.
- (19) Liu, X. M.; Lee, H. T.; Reinhardt, R. A.; Marky, L. A.; Wang, D. Novel Biomineral-Binding Cyclodextrins for Controlled Drug Delivery in the Oral Cavity. *J. Control. Release* **2007**, *122*, 54–62.
- (20) Saokham, P.; Loftsson, T. A New Approach for Quantitative Determination of  $\gamma$ -Cyclodextrin in Aqueous Solutions: Application in Aggregate Determinations and Solubility in Hydrocortisone/ $\gamma$ -Cyclodextrin Inclusion Complex. *J. Pharm. Sci.* **2015**, *104*, 3925–3933.
- (21) Jozwiakowski, M. J.; Connors, K. A. Aqueous Solubility Behavior of Three Cyclodextrins. *Carbohydr. Res.* **1985**, *143*, 51–59.
- (22) József Szejtli. *Cyclodextrin Technology*; Kluwer Academic Publishers: Dordrecht, 1988; p 13.
- (23) Yalkowsky, S. H. *Solubility and Solubilization in Aqueous Media*; Oxford University Press: New York, 1999; p 337.
- (24) Schwarz, D. H.; Engelke, A.; Wenz, G. Solubilizing Steroidal Drugs by  $\beta$ -Cyclodextrin Derivatives. *Int. J. Pharm.* **2017**, *531*, 559–567.